Fluorescence Study on Translational Mobility in Polystyrene–Polyethyleneglycol Microbeads

B. Lehr,[1] H.-J. Egelhaaf,[1] W. Rapp,[2] E. Bayer,[1] and D. Oelkrug[1]

Polyethyleneglycol (PEG) chain mobility in gelatineous microbeads is investigated by means of dynamic excimer formation. Pyrenebutyric acid (PYB) is covalently linked to the chain ends as probe molecule. Excimer formation is monitored by steady-state and time-resolved fluorescence spectroscopy in the presence of a series of liquid phases and in the dry state. PYB concentration in the beads is varied over three orders of magnitude up to $c = 6 \cdot 10^{-2}$ M. The concentration is derived from absorption measurements in stirred bead suspensions, considering the deviations from Lambert–Beer's law in heterogeneous systems. Excimer formation is found to be a dynamic process in the presence of liquid phases which solvate both the polymer and the fluorophore. The collisional rate constant, k_{DM}, is of the order of k_{DM}-values of PYB in homogeneous solutions, indicating a high translational mobility. Excimer-to-monomer intensity ratios are in general accordance with the solvation capacity of the liquid phase. In the dry state excimer formation is found only at high PYB concentrations, $c \approx 3 \cdot 10^{-2}$ M. It is concluded that this excimer emission arises from aggregated PYB, since corresponding fluorescence response curves show no rise time.

INTRODUCTION

Synthetic copolymers have become important solid supports in synthetic and analytical chemistry and chromatography. A typical copolymer representative is gel-type microspheres consisting of low cross-linked polystyrene (PS) grafted with polyethyleneglycol (PEG) chains [1,2]. When the microspheres are dispersed in a liquid, the polymer components are partly solvated and thus form a so-called "interphase," where reactions, specific interactions, and chromatographic separations take place. The requirements for practical application are high diffusion and reaction rates within the interphase, good accessibility of the reactive groups, and high capacity of the solid support.

Absorption and fluorescence spectroscopy are widespread tools for the investigation of polymers. Many of these materials will form inhomogeneous systems if the polymer is not completely solvated by the liquid phase. In this case optical spectroscopy is more difficult than in homogeneous solutions because the optical properties of the sample interfere with those of the chromophore itself, e.g., fluorescence anisotropy is partly depolarized by light scattering or absorption is dependent on the particle size, leading to deviations from Lambert–Beer's law.

In this work the fluorescence probe technique is applied to PS-PEG microspheres with diameters $d = 90\mu m$. The polymer structure is illustrated in Fig. 1. As probe molecule pyrenebutyric acid (PYB) is covalently linked to the PEG chain ends, pyrene and its derivatives

[1] Institute of Physical Chemistry, University of Tübingen, Tübingen, Germany.
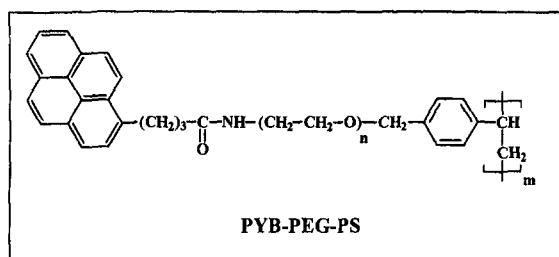[2] Rapp Polymere GmbH, Tübingen, Germany.

are able to form fluorescent excimers in a diffusion process and therefore have been used to probe the viscosity in synthetic copolymers, on chromatographic phases, and in biological material, e.g., membranes, micelles, and proteins [3–12].

The translational mobility of PYB-linked PEG chain ends is quantified by time-resolved fluorescence measurements of samples of different concentrations. We expect the collisional rate constant for excimer formation to be dependent on the liquid phase. A fluorescence anisotropy study on PEG-PS/liquid interphases revealed the strong influence of the liquid phase on the rotational mobility of chemically linked diphenylhexatrienylpropionic acid [13].

The PYB concentration is derived from absorption measurements in samples, where Lambert–Beer's law is not valid. According to the theory of absorption of heterogeneous systems, which describes the absorption as a function of particle size, the fluorophore concentration can be obtained only by absorption spectra in low-absorbing particles. This is possible with PYB as the chromophore over a wide concentration range, due to PYB's absorption bands differing in coefficient of absorption by a factor 50.

EXPERIMENTAL

The functionalization of PS-PEG microspheres [14] with PYB (Molecular Probes) was performed by shaking the beads in a dry dichloromethane solution of PYB (esterified with hydroxybenzotriazol). Different degrees of functionalization were obtained by varying the shaking time and the PYB concentration. After filtration the beads were thoroughly washed in dichloromethane, methanol, and diethyl ether and dried in vacuum. The functionalization capacity of the beads was 0.2–0.3 mmol/g.

Absorption measurements were carried out on a Lambda 2 spectrometer (Perkin Elmer). Decadic extinction coefficients of PYB in solution were found to be $\varepsilon = 44,000\ M^{-1}\ cm^{-1}$ for the L_a band and $\varepsilon = 800\ M^{-1}$ cm^{-1} for the L_b band. Absorption spectra of the beads were obtained by stirring the beads in commercial cuvettes to avoid sedimentation. Solvents were of spectroscopic grade.

Fluorescence spectra were performed on a Spex Fluorolog 222 spectrometer equipped with two double monochromators. All samples were purged with gaseous nitrogen prior to measurement at room temperature. I_E/I_M ratios were calculated by dividing the emission intensity at $\nu = 20,400\ cm^{-1}$ by the intensity at $\nu = 26,600\ cm^{-1}$.

Fluorescence decay times were obtained using the single-photon counting method [15,16]. As excitation source, a thyrathron-controlled nanosecond flashlamp was used. Excimer emission was monitored at $\nu = 20,000\ cm^{-1}$; monomer emission, at $\nu = 25,100\ cm^{-1}$. Biexponential deconvolution fits yielded decay times τ_i with an error of $\leq 5\%$ and preexponential factors A_i with an error of $\leq 10\%$ of the given data. Average fluorescence lifetimes $\langle \tau \rangle$ were calculated according to $\langle \tau \rangle = (A_1 \cdot \tau_1^2 + A_2 \cdot \tau_2^2)/(A_1 \cdot \tau_1 + A_2 \cdot \tau_2)$.

## RESULTS AND DISCUSSION

Absorption Spectra

Absorption measurements of five samples of different PYB concentration were carried out in stirred suspensions of typically 10 mg PYB-PEG-PS particles in 2.5 ml liquid phase. Results are shown in Fig. 2. The analysis requires insight into the theory of absorption of heterogeneous systems. The coefficient of absorption K of a liquid containing absorbing, spherical, monodispersed particles is described as follows [17–19]:

$$K = (3\varphi\ /\ 2d) \cdot \ln\ [1 - (P\ /\ \varphi)(1 - T)] \qquad (1)$$

In this equation, d is the particle diameter and P the packing density, defined as $P = N \cdot V/V_{liq}$, where N is the number of particles, V the volume occupied by a single particle, and V_{liq} the volume occupied by the liquid. φ is the theoretical maximum packing density and T the transmittance of a single spherical particle, derived by Duyckaerts [18]:

$$T = (2\ /\ (kcd)^2) \cdot [1 - (1 + kcd) \cdot \exp\ (-kcd)] \qquad (2)$$

k is the natural coefficient of absorption of the fluorophore, c the concentration of the fluorophore within the particles, and d the particle diameter.
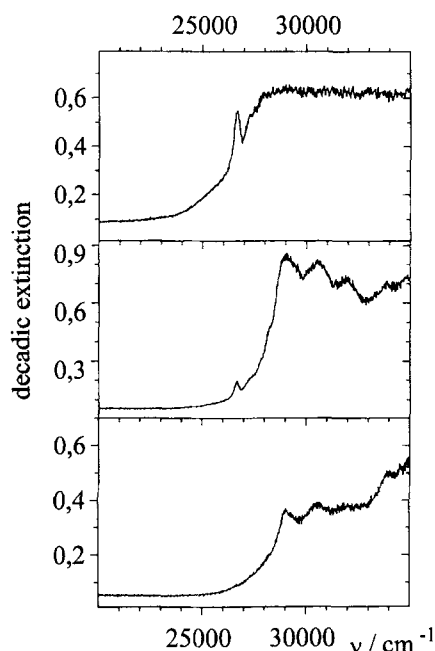
Fig. 2. Absorption spectra of PYB-PEG-PS microbeads dispersed in toluene. Reference: toluene. Top, $c_{PYB} = 6.10^{-2}\ M$; middle, $c_{PYB} = 4.10^{-3}\ M$; bottom, $c_{PYB} = 8.10^{-4}\ M$.

Table I. PYB Concentration c in Toluene-Swollen PYB-PEG-PS Particles and Monomer Fluorescence Decay Times, Obtained from Initial Slopes

Sample	c (M)	τ (ns)
I	$6 \cdot 10^{-2}$	12
II	$3 \cdot 10^{-2}$	—[a]
III	$4 \cdot 10^{-3}$	58
IV	$8 \cdot 10^{-4}$	59
V	$5 \cdot 10^{-5}$	106

[a] Not measured.

The meaning of these equations can be figured out by considering an extreme situation where P values are very low ($P \le 0.02$). Equations (1) and (2) yield an approximation of high absorption ($T \to 0$) $K = 3P/2d$, i.e., the absorption will be independent of the concentration but dependent on the particle size.

In the opposite case of low kcd values (and low P values), K can be approximated to $K = 3Pkc/2$. Here the absorption is independent of the particle size and proportional to the concentration of the fluorophore as is the case in molecular dispersions of fluorophores in homogeneous solutions. Between these two extreme situations the extinction increases nonlinearly with concentration.

In order to extract the PYB concentration, the absorption coefficient k in Eq. (2) is considered as the sum of the absorption coefficient of PYB plus the coefficient of all other contributions to the measured extinction, namely, the absorption of PEG-PS particles themselves and the light scattering of the sample. Absorption and scattering are additive as long as photons undergo only single scattering events. In the experiments, scattering is effectively reduced by keeping P values low and by choosing toluene as a refractive index matching liquid phase.

The limiting case of totally absorbing spheres ($T \to 0$) applies to the highest concentrated samples at wavenumbers $\nu \ge 28{,}000$ cm^{-1}. This situation is shown in sample I in Fig. 2 (top). Only the 0–0-peak of the L_b band at 26,800 cm^{-1} can be resolved because of its very low absorption coefficient. The spectrum saturates completely in the region of the strongly absorbing L_a band ($\nu > 28{,}000$ cm^{-1}). The very weak absorption onset at $\nu \ge 24{,}000$ cm^{-1} is assigned to small amounts of static pyrene aggregates with excimer-like fluorescence emission (compare the fluorescence excitation spectrum of sample I in Fig. 6).

In sample III, with a lower PYB concentration, the L_a band at $\nu = 29{,}100$ cm^{-1} is clearly resolved. The L_b band absorbs very weakly, while the aggregate band disappears (Fig. 2, middle). The absorption spectrum of sample IV is already distorted by the self-absorption of the PEG-PS polymer (Fig. 2, bottom). The pyrene concentrations of samples I–V dispersed in toluene are calculated from the experimental spectra (Fig. 2), the background spectrum (not shown), the molar absorption of PYB in homogeneous solution, and Eqs. (1) and (2). The results are listed in Table 1.

Fluorescence Spectra

Steady-state emission spectra of PYB provide the ratio of excimer emission intensity to that of the monomer, I_E/I_M, a measure for the aggregation of the fluorophores. I_E/I_M ratios in PYB-PEG-PS microspheres were found to be dependent on the fluorophore concentration as well as dependent on the present liquid phase.

I_E/I_M ratios depending on the liquid phase were best obtained from spectra of PYB-PEG-PS at $c = 4 \cdot 10^{-3}\ M$ (sample III). Fluorescence spectra of the lower concentrated sample IV show the same effect but with lower I_E/I_M ratios.

Figure 3 presents a selection of fluorescence spectra of sample III dispersed in liquid phases. All curves intersect at $\nu = 22{,}200$ cm^{-1} when normalized to equal integrals. This "isostilbic" point [20] appears in fluo-
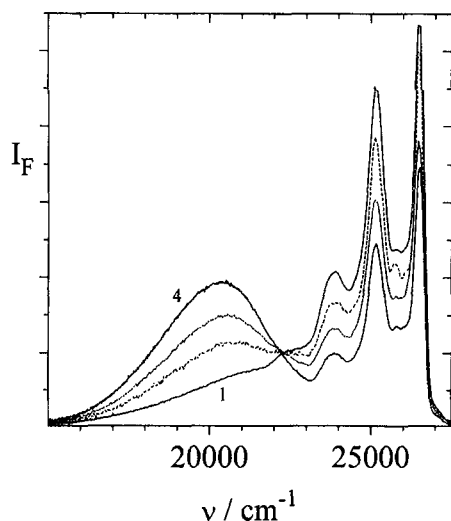
Fig. 3. Fluorescence spectra of PYB-PEG-PS microbeads (sample III) in the presence of different liquid phases, normalized to equal integral. (1) Cyclohexane; (2) ethanol; (3) toluene; (4) dichloromethane.
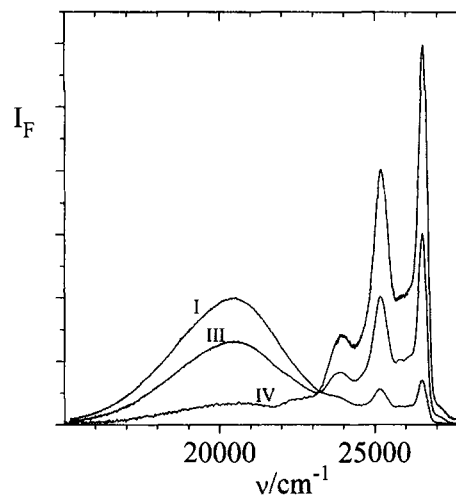

Fig. 4. Fluorescence spectra of PYB-PEG-PS in the presence of acetonitrile at different PYB concentration, normalized to equal integral. Sample I, $c = 6.10^{-2}$ M; sample III, $c = 4.10^{-3}$ M; sample IV, $c = 8.10^{-4}$ M.

Table II. I_E/I_M Ratios and Swelling Volumes of PYB-PEG-PS Microspheres (Sample III) in Several Liquid Phases

Liquid phase	I_E/I_M ratio	Swelling volume (ml/g)
Dichloromethane	0.56	5.1
Acetonitrile	0.56	5.1
Toluene	0.40	5.7
Ethanol	0.23	2.1
Diethyl ether	0.16	1.7
Cyclohexane	0.12	1.7
Water	0.08	4.3
Dry	0.15	1.7

rescence spectra composed by only two components in mutual dependence. I_E/I_M ratios are listed in Table II together with the swelling volume of the beads in the corresponding liquid phases. In the presence of cyclohexane or diethyl ether, and in the dry beads, fluorescence spectra show the structured monomer emission, while very small traces of excimer emission are observed. In other liquid phases such as acetonitrile or dichloromethane, the relative excimer emission intensity is significantly higher.

Assuming that excimer emission is caused by a collisional process, the factors determining the excimer emission intensity at a given temperature will be the PYB concentration, the translational diffusion of the PEG chain ends, i.e., the degree of solubilization of the PEG chains by the liquid phase, and the viscosity of the liquid phase. The I_E/I_M ratios are in general accordance

with the swelling volume, with the exception of water. In the dry state or in the presence of a liquid phase that is not able to penetrate into the beads, PYB is completely attached to the polymer, because the PEG chains stick together by van der Waals forces. Thus dynamic excimer formation is suppressed. In the presence of a liquid phase that is able to solvate both the PEG chains and the fluorophore, PYB gains translational mobility. In water, a bad solvent for hydrophobic molecules, PYB remains attached to the polymer.

As illustrated in Fig. 4, I_E/I_M ratios increase in acetonitrile swollen particles with increasing PYB concentration. Again, the spectra intersect at an isostilbic point.

Concentration-dependent fluorescence emission spectra in the dry state are plotted in Fig. 5. While at $c_{PYB} = 4 \cdot 10^{-3}$ M, only small amounts of excimer emission are observed, excimer emission dominates the spectrum at $c_{PYB} \geq 3 \cdot 10^{-2}$ M. At this concentration, large I_E/I_M ratios are observed in the dry beads as well as in acetonitrile dispersions. Figures 4 and 5 compare the fluorescence spectra of sample I in both environments. In the dry state the excimer emission is slightly structured and somewhat blue-shifted. Since the PYB concentration is very high, the question arises whether excimer emission originates at least partly from a static process. Several authors report on ground-state aggregation at high concentrations, e.g., of PYB chemically bound to controlled-pore glass [7] and of pyrene in membranes [21], in frozen solutions [22], and adsorbed on metal oxides [26].
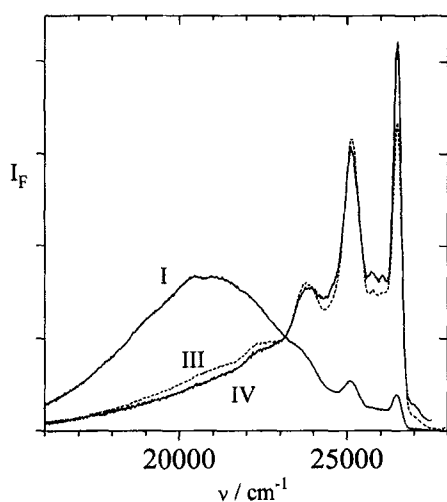
Fig. 5. Fluorescence spectra of PYB-PEG-PS in the dry state at different PYB concentrations normalized to an equal integral. Sample I, $c = 6.10^{-2}$ M; sample III: $c = 4.10^{-3}$ M; sample IV, $c = 8.10^{-4}$ M.

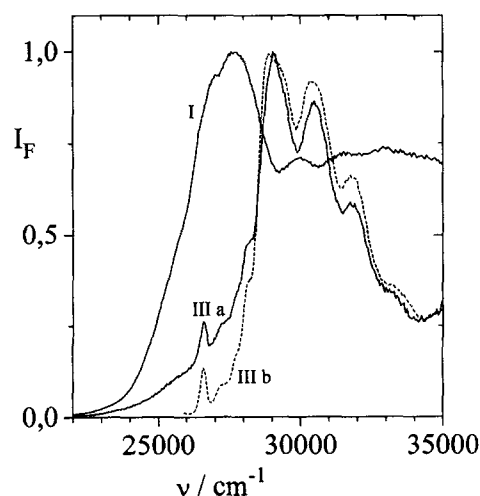**Fig. 6.** Fluorescence excitation spectra of PYB-PEG-PS in the presence of acetonitrile. Sample I, $\nu_{em} = 20,000$ cm^{-1}; sample III, (a) $\nu_{em} = 20,000$ cm^{-1} and (b) 25,000 cm^{-1}.

A test for ground-state aggregation is measuring fluorescence excitation spectra at both the excimer and the monomer emission wavelength. The spectra will not be superimposable if aggregates contribute to fluorescence. Figure 6 compares the excimer excitation spectra of samples I and III together with the monomer excitation spectrum of sample III in the presence of acetonitrile. While sample III shows mainly the monomer L_b and L_a bands, regardless of the emission wavelength, the excimer excitation spectrum of sample I is distorted by an inner filter effect. This leads to anticoincidence of the

absorption bands monitored at monomer and excimer emission wavelengths and provides evidence for a second absorbing species competing for the available light. This species is assigned to ground-state aggregates, as is frequently done in the literature [21,22,23].

The broad red-edge band at $\nu = 25,000$–$28,000$ cm^{-1} in sample I is caused to a large extent by static aggregates, but the apparent band maximum is an artifact due to the inner filter effect. In sample IIIa, the red edge of the absorption is still visible, but not in IIIb. Absorption of aggregates at the red edge of the excitation spectra was also observed by other authors [7,23].

So far, at high concentrations excimer emission is found even in swollen beads, due partly to aggregated PYB. However, from the observation of isostilbic points in both concentration- and liquid phase-dependent emission spectra we conclude that, in swollen beads, static excimers play only a minor role.

Fluorescence Decay Measurements

The time-dependent fluorescence emission profile of the excimer will present a rising component if emission originates from a dynamic process. Excimer formation of small molecules in solution is supposed to proceed according to Birks' mechanism [24]. The validity of the mechanism can be tested by the excimer emission time profiles, which must be formed by two exponentials with equal prefactors of opposite sign ($-A_1 = A_2$). The collisional rate constant k_{DM} of excimer formation can be calculated by

$$k_{DM} = \left(\frac{1}{\tau} - \frac{1}{\tau_0}\right) \cdot \frac{1}{C_{PYB}} \tag{3}$$

where τ is the monomer fluorescence decay time at a concentration of c_{PYB}, and τ_0 the monomer decay time in strongly diluted solution ($c_{PYB} \rightarrow 0$). For PYB we obtained collisional rate constants of $k_{DM} = 3 \cdot 10^9$ M^{-1} s^{-1} in ethanol and $k_{DM} = 7 \cdot 10^9$ M^{-1} s^{-1} in acetonitrile.

Figure 7 presents fluorescence decay curves of PYB-PEG-PS dispersed in acetonitrile, clearly showing a rising component for the excimer emission and thus proving dynamic excimer formation. Rising components are found in samples of $c_{PYB} = 8 \cdot 10^{-4}$ to $6 \cdot 10^{-2}$ M in the presence of acetonitrile and in sample III ($c_{PYB} = 8 \cdot 10^{-4}$ M) in the presence of liquid phases that solvate both the polymer and the fluorophore. These findings are in accordance with I_E/I_M ratios derived from steady-state emission spectra.

A selection of curve-fitting results is shown in Tables III and IV. Both monomer and excimer decays are
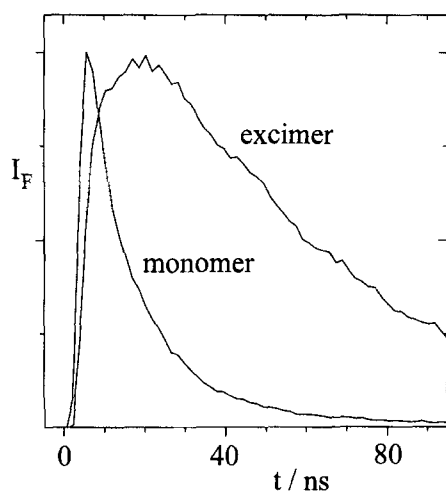
Fig. 7. Fluorescence decay curves of PYB-PEG-PS in the presence of acetonitrile measured at $\nu_{em} = 20,000$ cm^{-1} (excimer) and 25,000 cm^{-1} (monomer).

Table III. PYB-PEG-PS Fluorescence Decay Parameters of Sample III ($c = 4 \cdot 10^{-3}$ M): Decay times (τ), Relative Amplitudes (A), and Average Decay Times ($\langle\tau\rangle$) of Double-Exponential Fits

Liquid phase	τ_1 (ns)	A_1	τ_2 (ns)	A_2	$\langle\tau\rangle$ (ns)
Monomer emission					
Acetonitrile	37	0.73	94	0.27	64
Toluene	34	0.70	90	0.30	63
Ethanol	34	0.50	108	0.50	90
Cyclohexane	38	0.50	121	0.50	101
Dry	30	0.45	121	0.55	105
Excimer emission					
Acetonitrile	33	−0.39	59	0.61	
Toluene	28	−0.35	67	0.65	
Ethanol	34	−0.38	86	0.62	
Cyclohexane	19	0.52	87	0.48	
Dry	18	0.58	90	0.42	

Table IV. PYB-PEG-PS Fluorescence Decay Parameters of Sample I ($c = 6 \cdot 10^{-2}$ M): Decay Times (τ) and Relative Amplitudes (A) of Double-Exponential Fits

Liquid phase	τ_1 (ns)	A_1	τ_2 (ns)	A_2
Monomer emission				
Acetonitrile	12	0.96	23	0.04
Dry	21	0.61	55	0.39
Excimer emission				
Acetonitrile	12	−0.37	46	0.63
Dry	15	0.38	59	0.62

nonexponential, regardless of the present liquid phase. The curves were fitted with two exponentials. Triple-exponential fitting did not significantly enhance the quality of the fits. A nonexponential monomer decay is not surprising, because PYB's polymeric environment is not homogeneous. In the literature, nonexponential monomer decays in heterogeneous media are frequently reported, e.g., for pyrene adsorbed on silica gel [25] and chemically bound to lipid bilayers [10]. Compared to this, other possible contributions to nonexponential behavior like excimer dissociation or restricted translational diffusion are not clearly observable.

Qualitatively, the monomer decay times follow Eq. (3), which predicts decreasing decay times with increasing concentration and increasing collisional rates. The monomer τ_2 values in sample III increase going from acetonitrile to cyclohexane, while simultaneously their preexponential factors become smaller. However, τ_2 values do not change significantly.

Apart from a rising component, the excimer decay should reflect the monomer decay time in one of the two τ values. This is the case in sample I, where the excimer τ_2 value and the monomer decay are equal. Here the monomer decay is nearly exponential. This feature is not so obvious in sample III, where monomer decays are by far nonexponential. The monomer τ_1 values are roughly the same as the excimer τ_1 values. However, the average monomer decay times $\langle\tau\rangle$ correspond with excimer τ_2 values.

The ratios of the excimer preexponential factors, $-A_1/A_2$, deviate from unity. This is obviously due to ground-state aggregates contributing to the excimer emission at $\nu = 20,000$ cm^{-1} even in swollen beads.

From the discussion above, it is clear that the application of Eq. (3) is only an approximation. Taking the monomer τ values from the initial slopes of the decay curves (see Table I), we obtain k_{DM} values between $1 \cdot 10^9$ and $9 \cdot 10^9$ M^{-1} s^{-1} for the different samples. Though these results are only approximate, we can interprete these values as an indication of high translational mobility.

CONCLUSION

PEG chain mobility in gel-type PS-PEG microspheres is probed by excimer formation of covalently linked PYB. Using the theory of absorption in heterogeneous systems, the PYB concentration is determined by absorption measurements of bead suspensions in liquid phases.

Excimer formation is found to be a dynamic process when the beads are dispersed in liquid phases that solvate both the polymer and the probe molecule. Collisional rates in the presence of acetonitrile are of the order of collisional rates in homogeneous solutions, indicating a high translational mobility. However, dynamic excimer formation is accompanied by ground-state aggregation of pyrene, even in swollen beads. No dynamic excimers are observed in the dry state and in the presence of liquid phases that do not solvate the polymer. In these systems, only static aggregates are found.

ACKNOWLEDGMENTS

REFERENCES

1. E. Bayer and W. Rapp (1992) in J. M. Harris (Ed), *Poly(Ethylene Glycol) Chemistry: Biotechnical and Biomedical Applications*, Plenum Press, New York.
2. E. Bayer (1991) *Angew. Chem. Int. Ed. Engl.* **30**, 113–129.
3. F. M. Winnik (1993) *Chem. Rev.* **93**, 587–614.
4. H. Evertsson and S. Nilsson (1997) *Macromolecules* **30**, 2377–2385.
5. H. Mihara, J. Hayashida, H. Hasegawa, H. Ogawa, T. Fujimoto, and N. Nishino (1997) *J. Chem. Soc. Perkin Trans.* **2**, 517–522.
6. K. Ebata, M. Masuko, H. Ohtani, and M. Kashiwasake-Jibu (1995) *Photochem. Photobiol.* **62**(5), 836–839.
7. J. Zilberstein, A. Bromberg, and G. Berkovic (1994) *J. Photochem. Photobiol. A Chem.* **77**, 69–81.
8. A. Ueno (1990) *Anal. Chem.* **62**, 2461–2466.
9. H. T. Oyama, W. T. Tang, and C. W. Frank (1987) *Macromolecules* **20**, 1839–1847.
10. H. Lemmetyinen, M. Yliperettula, J. Mikkola, J. A. Virtanen, and P. K. J. Kinnunen (1989) *J. Phys. Chem.* **93**, 7170–7175.
11. C. H. Lochmüller and T. J. Wenzel (1990) *J. Phys. Chem.* **94**, 4230–4235.
12. J. Stahlberg, M. Almgren, and J. Alsins (1988) *Anal. Chem.* **60**, 2487–2493.
13. B. Lehr, H.-J. Egelhaaf, H. Fritz, W. Rapp, E. Bayer, and D. Oelkrug (1996) *Macromolecules* **29**, 7931–7936.
14. The PEG-PS beads are called TentaGel, a trademark of Rapp Polymere GmbH, Tübingen.
15. A. E. W. Knight and B. K. Selinger (1973) *Aust. J. Chem.* **32**, 1–27.
16. A. J. Cross and G. R. Fleming (1984) *Biophys. J.* **46**, 45–56.
17. B. Felder (1964) *Helv. Chim. Acta* **47**, 488–497.
18. G. Duyckaerts (1955) *Spectrochim. Acta* **7**, 25–31.
19. G. Kortüm and D. Oelkrug (1966) *Naturwissenschaften* **53**, 600–609.
20. T. Förster (1969) *Angew. Chem.* **81**, 364–374.
21. M. F. Blackwell, K. Gounaris, and J. Barber (1986) *Biochim. Biophys. Acta* **858**, 221–234.
22. E. Loewenthal, Y. Tomkiewicz, and A. Weinreb (1969) *Spectrochim. Acta* **25A**, 1501–1513.
23. M. Szadowska-Nicze, M. Wolszczak, J. Kroh, and J. Mayer (1993) *J. Photochem. Photobiol. A Chem.* **75**, 125–129.
24. J. B. Birks (1970) *Photophysics of Aromatic Molecules*, John Wiley, New York.
25. R. K. Bauer, P. de Mayo, W. R. Ware, and K. C. Wu (1982) *J. Phys. Chem.* **86**, 3781–3789.
26. D. Oelkrug, M. Radjaipour, and H. Erbse, *Z. Phys. Chem. N.F.* (1974) **88**, 23–36.